Genomics 117 (2025) 111124

Contents lists available at ScienceDirect

Genomics

journal homepage: www.elsevier.com/locate/ygeno

Genome-wide association study identifies novel candidate genes linked to acute and chronic thermal stress resilience in olive flounder (*Paralichthys olivaceus*)

H.A.C.R. Hanchapola [a,1], Po Gong [a,b,1], Gaeun Kim [a,c,1], D.S. Liyanage [a,c], W.K.M. Omeka [a,c], Jeongeun Kim [a,c], Yasara Kavindi Kodagoda [a], M.A.H. Dilshan [a], D.C.G. Rodrigo [a], G.A.N. Piyumika Ganepola [a], Cecile Massault [d], Dean R. Jerry [d,e], Jihun Lee [a,c,*], Jehee Lee [a,c,*]

[a] Department of Marine Life Sciences & Center for Genomic Selection in Korean Aquaculture, Jeju National University, Jeju 63243, Republic of Korea
[b] Marine Life Research Institute, Jeju National University, Jeju 63333, Republic of Korea
[c] Ocean and Fisheries Research Institute, Jeju Self-Governing Province, 63629, Republic of Korea
[d] Centre for Sustainable Tropical Fisheries and Aquaculture, College of Science and Engineering, James Cook University, Townsville, QLD 4811, Australia
[e] Tropical Futures Institute, James Cook University, Singapore

ARTICLE INFO

Keywords:
Genome-wide association study
Olive flounder
Single nucleotide polymorphism
Thermal stress

ABSTRACT

Acute and chronic high-temperature stress negatively impact olive flounder (*Paralichthys olivaceus*) aquaculture, weakening immune function and increasing mortality. This study conducted a genome-wide association study (GWAS) to identify genetic markers linked to thermal stress resilience. A total of 384 fish were exposed to acute stress (29 °C for 30 min and 1 h) and chronic stress (19.8–30 °C for 16 days). Genomic DNA from 329 deceased and 55 surviving fish was genotyped using a 70 K SNP chip, yielding 57,638 SNPs from 376 fish after quality filtering. GWAS identified 34 SNPs associated with both acute and chronic thermal stress on chromosomes 4, 10, 11, 15, 18, 19, and 23, surpassing the suggestive ($p < 1 \times 10^{-4}$) and Bonferroni-corrected ($p < 8.6 \times 10^{-7}$) thresholds. Genes *myhc*, *nlrc5*, *hydin*, and *gfod1* were linked to thermal stress. These findings may support marker-assisted selection for thermal stress resilience strains, promoting sustainable aquaculture.

1. Introduction

Olive flounder (*Paralichthys olivaceus*), renowned for its delicate flavor and high economic value, is a commercially dominant fish species in global aquaculture. Owing to decades of research and the development in intensive aquaculture techniques, South Korea has become the leading producer of olive founder, accounting for over half of global production [1]. Therefore, this species plays a critical role in South Korea's aquaculture industry. Both acute and chronic high-temperature stress, owing to environmental fluctuations, particularly rising water temperatures, pose as major challenges to olive flounder aquaculture. These stressors stemming from transportation, varying dissolved oxygen (DO) levels, tank design, and climate change disrupt essential physiological processes in this species. Elevated temperatures also compromise the immune system of olive flounders, leading to reduced growth rates and increased mortality [2]. Cortisol, a stress hormone, plays a crucial role in the fish's response to thermal stress. Therefore, understanding the genetic mechanisms of cortisol regulation and the survival of this species under high-temperature conditions is essential for improving aquaculture practices [3].

Genome-wide association studies (GWAS) have become increasingly important in aquaculture research, benefiting olive flounder and other commercially important species. For example, GWAS have been employed to clarify the genetic basis of thermal stress tolerance in Atlantic salmon (*Salmo salar*) [4,5] European sea bass (*Dicentrarchus labrax*) [6], and zebrafish (*Danio rerio*) [7–10], highlighting a complex interaction between heat shock proteins, immune response elements, and endocrine regulation. For olive flounder, researchers have employed high-density single nucleotide polymorphism (SNP) markers in GWAS to explore various traits, including growth performance [11], viral hemorrhagic septicemia virus (VHSV) resistance [12], and thermal stress tolerance [13]. However, the integration of the levels of stress

* Corresponding authors at: Marine Molecular Genetics Lab, Jeju National University, 102 Jejudaehakno, Jeju 63243, Republic of Korea.
E-mail addresses: jihun137@jejunu.ac.kr (J. Lee), jehee@jejunu.ac.kr (J. Lee).
[1] These authors contributed equally to this work.

https://doi.org/10.1016/j.ygeno.2025.111124
Received 24 March 2025; Received in revised form 8 August 2025; Accepted 29 September 2025
Available online 30 September 2025

hormones, such as cortisol, as a trait of interest in GWAS is still a relatively novel approach with the potential to offer in-depth understanding regarding the physiological mechanisms underlying stress resilience.

The primary objective of this study was to identify the genetic variants associated with both acute cortisol responses and chronic thermal tolerance in olive flounder using GWAS. We hypothesized that specific genetic polymorphisms within the genome of olive flounder drive individual variations in cortisol regulation and thermal stress tolerance. Therefore, cortisol levels were measured in individuals following acute high-temperature exposure, and the same fish were subsequently exposed to chronic high-temperature conditions to assess survival. Through this approach, SNPs significantly associated with both cortisol response and survival following chronic thermal exposure were identified. The findings of this study provide insights into the genetic mechanisms underlying both acute and chronic thermal stress adaptation in olive flounder, and the identified markers may serve as potential targets for selective breeding programs aimed at improving thermal resilience in olive flounders.

2. Methodology

2.1. Fish population and progeny information

The parental generation for obtaining the dF0 generation consisted of three groups—oF0, JJ, and WD groups. The oF0 group comprised 100 males and 110 females, while the JJ and WD groups comprised 70 and 57 females, respectively. dF0 offspring were produced by crossbreeding selected parent fish from a broodstock of 192 female and 74 male olive flounders. The breeding was conducted in October 2022 at the Haeyeon hatchery, Jeju, South Korea, in accordance with standard commercial procedures. For strip spawning, 16 groups, each comprising dams and sires, were established, ensuring that the genetic relatedness between parents of opposite sexes and between individuals of the same sex did not exceed 0.15 and 0.25, respectively. Eggs and sperms were manually collected and mixed at a ratio ranging from 1:3 to 1:5 to facilitate fertilization [14]. The resulting progeny were reared in the nursery for 185 days post-fertilization, reaching an average body weight of 63.44 ± 12.3 g and an average total length of 18.48 ± 1.5 cm. Subsequently, a total of 1200 fish were transferred to a 2000 L tank at the Jeju Special Self-Governing Province Ocean and Fisheries Research Institute. There, they were acclimated to a temperature range of 19–21 °C in a system equipped with continuous aeration and sand-filtered seawater. The fish were reared for 8 months prior to the experiment and were fed commercial extruded pellet (Daebong LF, Korea) twice daily until 2 days before the experiment during the acclimatization period.

2.2. Acute thermal challenge, blood sample collection, and serum separation

After a three-week acclimation period, the fish were distributed into four 500-L tanks, with approximately 146 fish per tank, for acute high-temperature exposure experiments. A total of 576 fish (average weight, 591.31 ± 1.4 g; average length, 37.21 ± 3.0 cm; and average width, 14.31 ± 1.3 cm) were directly exposed to a temperature of 29 °C for 30 min. Thereafter, blood samples (3 mL) were collected from the caudal veins of the fish using a needle syringe and the fish were returned to the same tanks for another acute high-temperature exposure experiment at 29 °C for 1 h. After the 1 h exposure step, blood samples (3 mL) were again collected from the caudal veins of the fish using the same procedure. Throughout the experiment, tank temperatures, maintained using a heating ventilation system, were monitored using both electronic and alcohol-based thermometers.

The collected blood samples were stored at 4 °C for 24 h to allow clotting. Subsequently, serum samples were isolated by centrifugation at 1300 ×g for 10 min at 4 °C and stored at −80 °C until further analysis.

2.3. Chronic thermal challenge and sampling

The same experimental groups as described in Section 2.2 were used for the chronic thermal tolerance experiment. Following blood collection after the acute thermal stress exposure experiment, the fish were acclimated for 3 weeks at the Marine Fishery Research Institute, Pyeoseon-Jeju, South Korea. During acclimation, the water temperature and dissolved oxygen level were maintained at 19.4 ± 0.5 °C and above 90 %, respectively. Thereafter, the temperature was gradually increased to 28 °C at a rate of 2 °C per day and then to 30 °C at a rate of 1 °C per day and maintained until the end of the experiment.

During the experiment, dead fish were removed hourly, and their fins were collected and stored at −80 °C for subsequent genomic DNA (gDNA) extraction. Additionally, at the end of the chronic exposure experiment, fin samples were collected from surviving fish and stored under the same conditions for gDNA extraction. Morphometric measurements, including weight, length, width, and any deformities, were recorded for both dead and surviving fish, based on three traits defined as follows: (1) Survival, a binary trait indicating whether a fish died (0) or survived (1) until the end of the challenge period; (2) Days to death, defined as the number of days a fish survived during the experiment based on its time of death; and (3) Hours to death, defined as the number of hours a fish survived during the experiment until death. All the experiments performed on the test animals were reviewed and approved by the Animal Care and Use Committee of Jeju National University (approval numbers 2023–0034 and 2024–0006).

2.4. Cortisol level measurement using ELISA

A commercially available enzyme-linked immunosorbent assay (ELISA) kit (MyBioSource, San Diego, CA, USA) was used to measure cortisol levels in fish serum at two time points following acute high-temperature exposure experiments. The serum samples were diluted to 1:100 and all the reagents and working standards were prepared according to the manufacturer's instructions. The ELISA plate included blank wells that contained neither samples nor standards, while in each test well, 50 μL of standard or diluted sample was added, followed by the addition of 50 μL of antibody conjugate (diluted 1×).

The contents of each well were thoroughly mixed by pipetting or gentle shaking for 60 s and incubated for 40 min at 37 °C. Thereafter, they were aspirated and washed three times with 200 μL of wash buffer, and further incubated for 2 min. After the wash buffer was completely removed, 100 μL of HRP-conjugate (diluted 1×) was added to each well (excluding the blank wells) and the plates were then covered and incubated for 30 min at 37 °C. Next, the washing step was repeated five times using the wash buffer. Subsequently, 90 μL of TMB substrate was added to each well and incubation was again performed in the dark at 37 °C for 3–5 min. Finally, the reaction was stopped by adding 50 μL of stop solution to each well, and absorbance measurements were performed at 450 nm using a microplate spectrophotometer (Multiskan GO, Thermo Fisher Scientific, Waltham, MA, USA) at 25 °C within 5 min.

2.5. Genotyping and quality control

To isolate gDNA from the caudal fin tissues of the 384 experimental fish, the fin tissues (approximately 50 mg each) were preserved in 100 % ethanol and sent to Bluegen (Busan, South Korea) for gDNA extraction and genotyping using the Affymetrix® Axiom® myDesign™ 70 K SNP Genotyping Array. Specifically, genotype calling was performed using Axiom® Analysis Suite 4.0 software, which employs internal clustering algorithms. Quality control filtering was also performed in accordance with the recommended best practices workflow of the Axiom® Analysis Suite. Only samples meeting the criteria: dish quality control (DQC) values ≥0.82 and QC call rates ≥0.95 were retained for further SNP filtering. Additionally, during the SNP filtering process, several quality thresholds: minimum call rate (≥ 0.99), Fisher's linear discriminant

cluster separation (FLD) ≥ 5.2, heterozygous strength offset (HetSO) ≥ 0.01, and minor allele frequency (MAF) ≥ 0.05, were applied. This stringent filtering process yielded a high-quality genotypic dataset with an average call rate of 99.6 %. An additional quality control step was performed on the 384 dF0 fish using the PLINK 1.9 software (www.cog-genomics.org/plink/1.9/) [15] to ensure that the genotype call rate and MAF exceeded 0.90 and 0.05, respectively. Finally, the distributions and densities of the quality-controlled SNPs across the flounder genome were visualize using the CMplot R package [16].

2.6. Descriptive statistics, heritability estimation, and trait correlation

Descriptive statistics for body weight (BW), body length (BL), body height (BH), cortisol levels at 30 min (C30) and 1 h (C90), sex, date of death (DPC_date), time of death (DPC_time), and survival status (SUR) were obtained using R software (version 4.1.2).

Further, to determine additive genetic and residual effects for heritability calculations, the following mixed linear model was used:

$$Y = X\beta + Zu + e$$

where Y represents phenotype (C30, C90, DPC_date, DPC_time, and SUR), β denotes fixed effects (sex and first 10 principal component (PC) values), u represents additive genetic effects (assumed to be normally distributed with the mean 0 and variance G), e represents residual effects (assumed to be normally distributed), and X and Z represent the incidence matrices of the fixed and additive effects, respectively. The genomic relationship matrix (GRM) was calculated using the "gaston" package in R (https://rdocumentation.org/packages/gaston/versions/1.4.9).

Narrow-sense heritability (h^2) and the associated variances were also estimated using R packages, "gaston" and "heritability" [11], and heritability was calculated using the following equation:

$$h^2 = \frac{\sigma_A^2}{\sigma_A^2 + \sigma_E^2}$$

where σ_A^2 represents additive genetic variance and σ_E^2 represents residual variance.

Phenotypic correlations among traits were assessed using Pearson's correlation coefficient in R. Genetic correlations were further estimated using R package "gaston" (https://www.rdocumentation.org/packages/ga%20ston/versions/1.4.9) based on the following equation:

$$r_g = \frac{cov_g(X, Y)}{\sqrt{\sigma_{a.x}^2 \times \sigma_{a.y}^2}}$$

where $cov_g(X, Y)$ represents the genetic covariance between traits X and Y and $\sigma_{a.x}^2$ and $\sigma_{a.y}^2$ represent the additive genetic variances of traits X and Y, respectively.

2.7. Population structure and linkage disequilibrium (LD) analysis

Principal component analysis (PCA) was conducted in R to evaluate genetic similarity and determine the overall genetic structure of the test population. The analysis included genotype data from individuals who passed quality control filtering criteria. The genetic structure of the population was further visualized using the ggplot2 package (https://ggplot2.tidyverse.org) in R.

The SNP chip, with markers distributed across the genome of olive flounder was used to assess linkage disequilibrium (LD) within the population. Pairwise correlations between SNPs were also analyzed using PLINK 1.9 software. Then, to visualize LD decay, the squared correlation coefficient (r^2) for each SNP pair was plotted against their physical distance (in kilobases, kb). The r^2 values ranged from 0 to 1, with 0 indicating no LD (free recombination) and 1 indicating complete LD (little or no recombination).

2.8. Association analysis, SNP annotation, and candidate gene identification

The Gaston package and a mixed linear model (as described in Section 2.6) were utilized to conduct the GWAS and to account for polygenic effects, a GRM was employed to estimate additive genetic variances. Specifically, associations between individual SNPs and selected traits were determined using Gaston, employing methods, such as the Wald test, linear mixed model (LMM) approach and quantitative trait analysis [17]. Significant SNPs were then identified using the Bonferroni-adjusted significance threshold ($0.05/57{,}638 = 8.6 \times 10^{-7}$) and the suggestive significance threshold (1×10^{-4}) in line with previously reported GWAS analyses [18,19]. For visualization, Manhattan and quantile-quantile (QQ) plots were generated using the Gaston and qqman R packages (https://github.com/stephenturner/qqman). Further, the genomic inflation factor (λ) was estimated as previously outlined by Aslam et al., [20].

The ParOil_1.1 General Feature Format (GFF) file for olive flounder (Accession No: GCA_001904815.2) was used to obtain detailed genomic sequence information for identifying significant SNPs across various genomic regions, including intergenic, intronic, and exonic sequences. The extracted sequences were manually annotated using National Center for Biotechnology Information (NCBI) BLAST (Basic Local Alignment Search Tool; https://blast.ncbi.nlm.nih.gov/Blast.cgi). Specifically, for SNPs located in intragenic regions, candidate genes were defined as those located within the same LD block, spanning a window of ±21 kb surrounding the SNP. Additional comprehensive gene annotation was achieved by integrating GFF and FASTA files from the ParOil_1.1 reference data using SnpEff software (https://pcingola.github.io/SnpEff/) [16].

2.9. Functional annotation of candidate genes

The functional characterization of significant SNP-harboring genes identified by GWAS was performed using the Database for Annotation, Visualization, and Integrated Discovery (DAVID). First, the significant genes associated with these SNPs were first identified using the UniProt database (https://www.uniprot.org/). Thereafter, their unique identifiers were analyzed using DAVID (https://david.ncifcrf.gov/). Enriched gene ontology (GO) terms and pathways that met two criteria: a statistically significant p-value ($p < 0.05$) and the inclusion of at least two candidate genes, were also identified, and for visualization, bubble plots were generated using the Viridis R package (https://github.com/sjmgarnier/viridis).

3. Results

3.1. Descriptive statistics

Table 1 provides a summary of descriptive statistics regarding the effects of acute and chronic high temperature exposure on the different phenotypic traits of olive flounder. In this table, C30 and C90 capture the responses of olive flounder to acute high temperatures, whereas SUR, DPC_date, and DPC_time reflect the effects of chronic high temperatures. Chronic high-temperature exposure resulted in a cumulative mortality rate of 90.1 % and a survival rate of 9.9 %, as per the tank-specific fish mortality presented in supplementary Fig. 1.

3.2. Genotyping and SNP quality control

From the initial set of 576 collected samples, 384 were selected for genotyping; among them, 376 (324 from dead fish and 52 from survivors) that passed stringent QC filtering were retained for further analysis. These samples were genotyped using the PolyHighResolution probe

Table 1
Descriptive statistics for the phenotypes measured in the experimental population.

Trait	No of samples (QC filtered)	Minimum	Median	Max	Mean	SD (±)
Body Weight (g)	376	163	492.50	806	494.69	117.80
Body Length (cm)	376	23.70	35.90	44.50	35.81	2.88
Body Height (cm)	376	9.40	13.20	16.30	13.18	1.10
C30 (ng/ml)	376	41.68	62.19	81.42	62.19	6.81
C90 (ng/ml)	376	45.83	64.70	102.32	65.50	7.52
DPC_time (h)	376	12	63.50	162	76.02	46.28
DPC_date (days)	376	1	3	7	3.64	1.85

set, yielding 57,651 SNPs. Additional QC filtering resulted in a final set of 57,638 high-quality SNPs, which were then used for downstream analysis. The distribution of these SNPs across olive flounder chromosomes was non-uniform, with chromosomes 7 and 14 showing the highest and lowest SNP distribution densities, respectively (Fig. 1).

3.3. LD and population structure analysis

LD was investigated across the genotyped QC-filtered SNPs in the genome of olive flounder. A plot of LD decay against the physical distance (in kb) between SNP pairs revealed that the LD decayed to half its maximum value (1/2 LD) within 21 kb (Fig. 2A). The use of this decay distance to determine the minimum number of markers required for the experiment showed that at least 26,000 SNPs were needed to provide sufficient coverage for the 546 Mb genome.

Scree plot analysis to determine the optimal number of offspring clusters based on genetic variance identified three distinct populations (Fig. 2B), consistent with the GRM heat map results (Fig. 2C). Additionally, PCA of genotypic data to assess population structure and genetic relatedness among the offspring revealed that the first 10 principal components (PCs) accounted for 67.04 % of the total observed genetic variance, with PC1 and PC2 explaining 11.09 % and 9.92 % of the variation, respectively, underscoring their primary roles in defining the population structure (Fig. 3).

3.4. Genome-wide association analysis

GWAS was employed to investigate the association between SNPs and high-temperature stress responses in the experimental population. Based on Bonferroni correction (8.7×10^{-7}) and suggestive cutoff (1×10^{-4}) significance thresholds, 34 significant SNPs associated with C30, C90, SUR, DPC_date, and DPC_time were identified via a Manhattan plot. For acute high-temperature stress, three SNPs were associated with C30 (Fig. 4A) and four were associated with C90 (Fig. 4B) with the significance levels above the suggestive threshold, and for chronic high-temperature stress, two SNPs were associated with SUR with the significance level above the suggestive threshold (Fig. 4C), and three were associated with DPC_date (Fig. 4D) and four with DPC_time (Fig. 4E), with the significance level exceeding the Bonferroni threshold. A quantile-quantile (QQ) plot analysis yielded genomic inflation factors

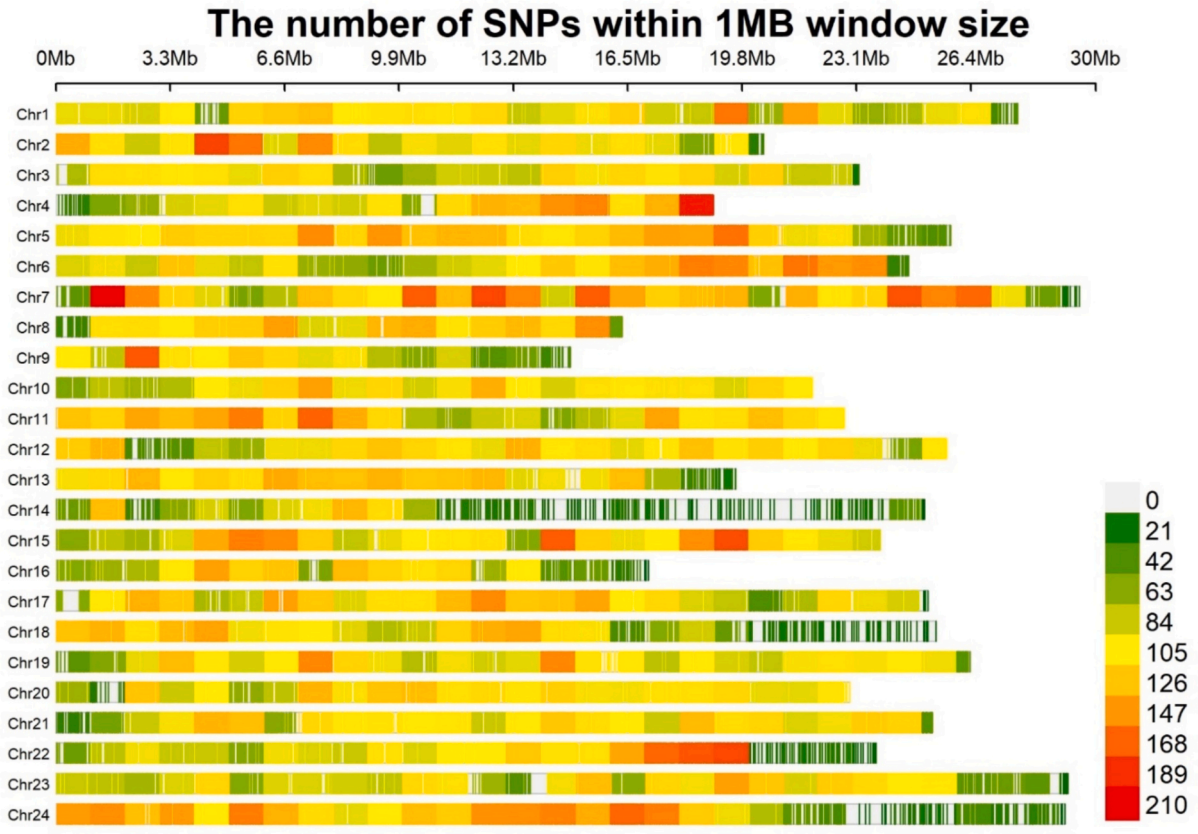

Fig. 1. Density and distribution of quality control (QC)-filtered SNPs across 24 chromosomes. The SNP density on each chromosome is denoted using the defined color scale.

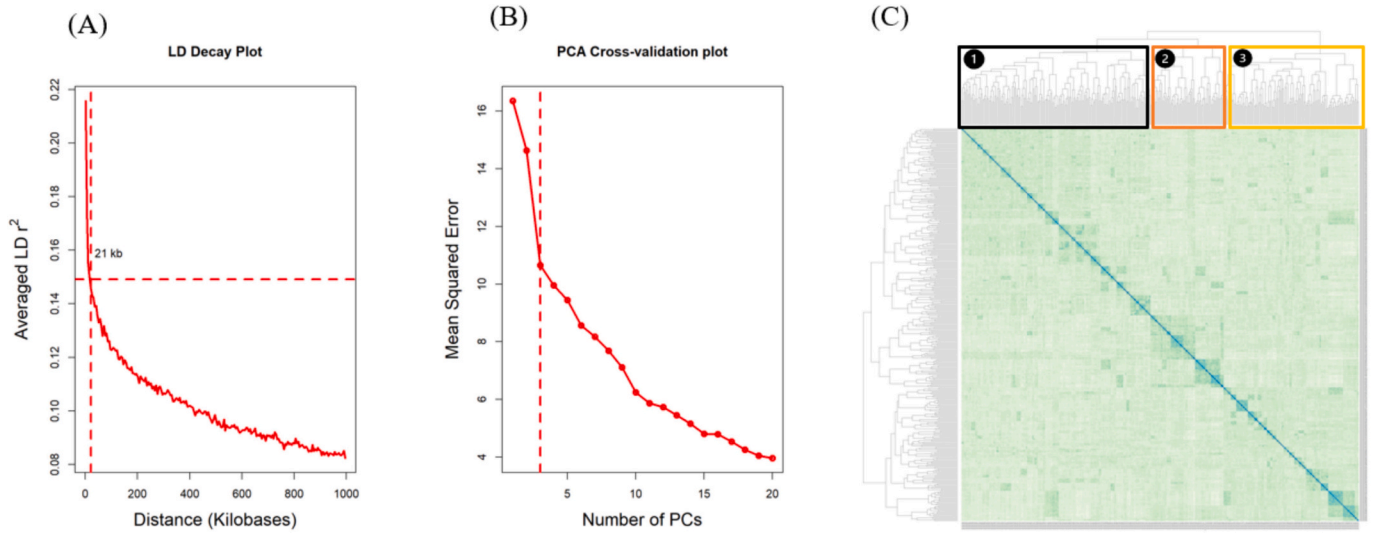

Fig. 2. (A) Linkage disequilibrium (r^2) decay as a function of distance (kilobases) for adjacent SNPs. Horizontal and vertical lines represent the half r^2 value as a measure of LD50 and the distance in kb between two alleles at LD50, respectively. (B) The scree plot of the principal component analysis (PCA). Vertical dash line representing the first bending point (elbow of the graph), where optimum number of population genetic structures are observed, and (C) Genomic relationship matrix (GRM) heat map.

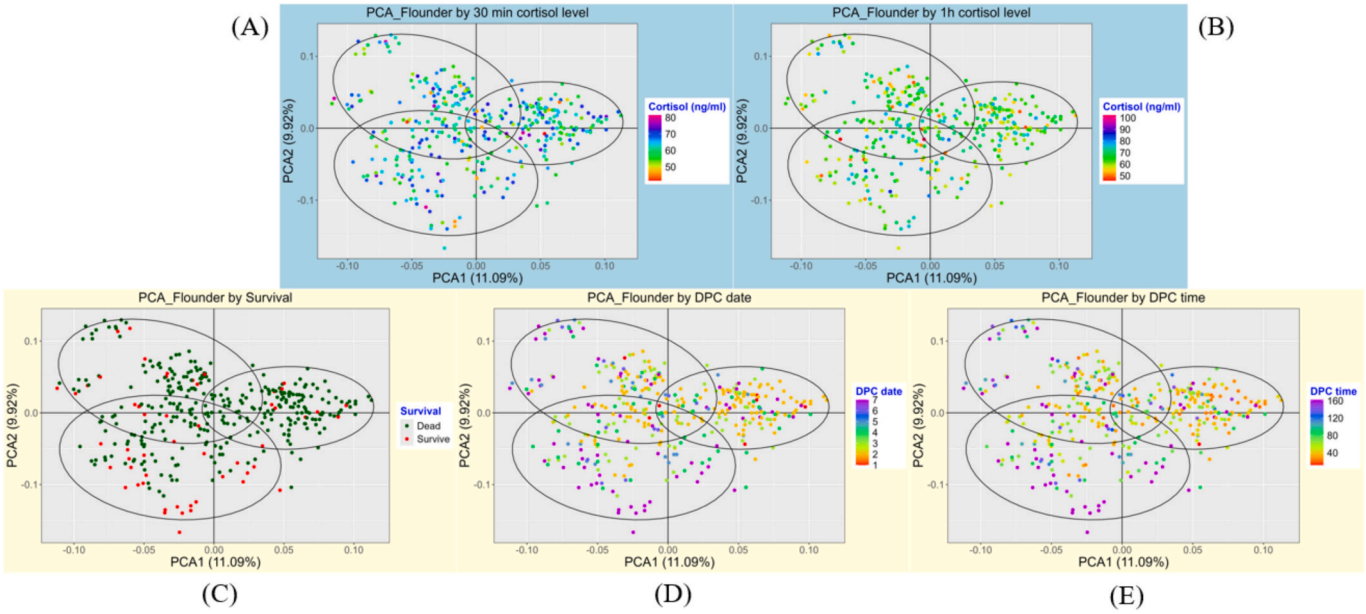

Fig. 3. Principal component analysis (PCA) of the acute and chronic high-temperature stress challenges. Panels display variations for (A) acute stress C30, (B) acute stress C90, (C) chronic stress survival, (D) chronic stress DPC_date, and (E) chronic stress DPC_time traits, as identified using the first two PCs. The three circles represent the distinct populations identified in the study.

(λ) of 0.910, 1.089, 1.073, 0.991, and 0.977 for C30, C90, SUR, DPC_date, and DPC_time, respectively, indicating minimal inflation of test statistics owing to unaccounted factors.

3.5. Heritability estimation and genotypic and phenotypic correlation

Heritability estimates for the five traits, determined using phenotypic and genotypic data, revealed higher heritability for chronic thermal stress traits than for acute thermal stress traits (Table 2). The phenotypic and genotypic correlations among all the considered traits were also examined. Thus, phenotypic correlation analysis revealed no association between C90 and DPC_date or DPC_time. However, a weak positive correlation (0.1) was observed between C90 and SUR, while strong correlations were observed between SUR and DPC_date (0.73) and between SUR and DPC_time (0.75). Additionally, DPC_date and DPC_time showed a very strong correlation (0.99), indicating strong concordance between these two death time measurements (Fig. 5A).

Similarly, genetic correlation analysis revealed weak associations between C90 and both SUR and DPC_time (0.01) and between C90 and DPC_date (0.02). However, the genotypic correlations between SUR and both DPC_date and DPC_time (both 0.71) were comparable to their phenotypic correlations, suggesting a genetic basis for the association between survival and time to death. Additionally, the genotypic correlation between DPC_date and DPC_time remained high (0.93), consistent with their phenotypic correlation (Fig. 5B).

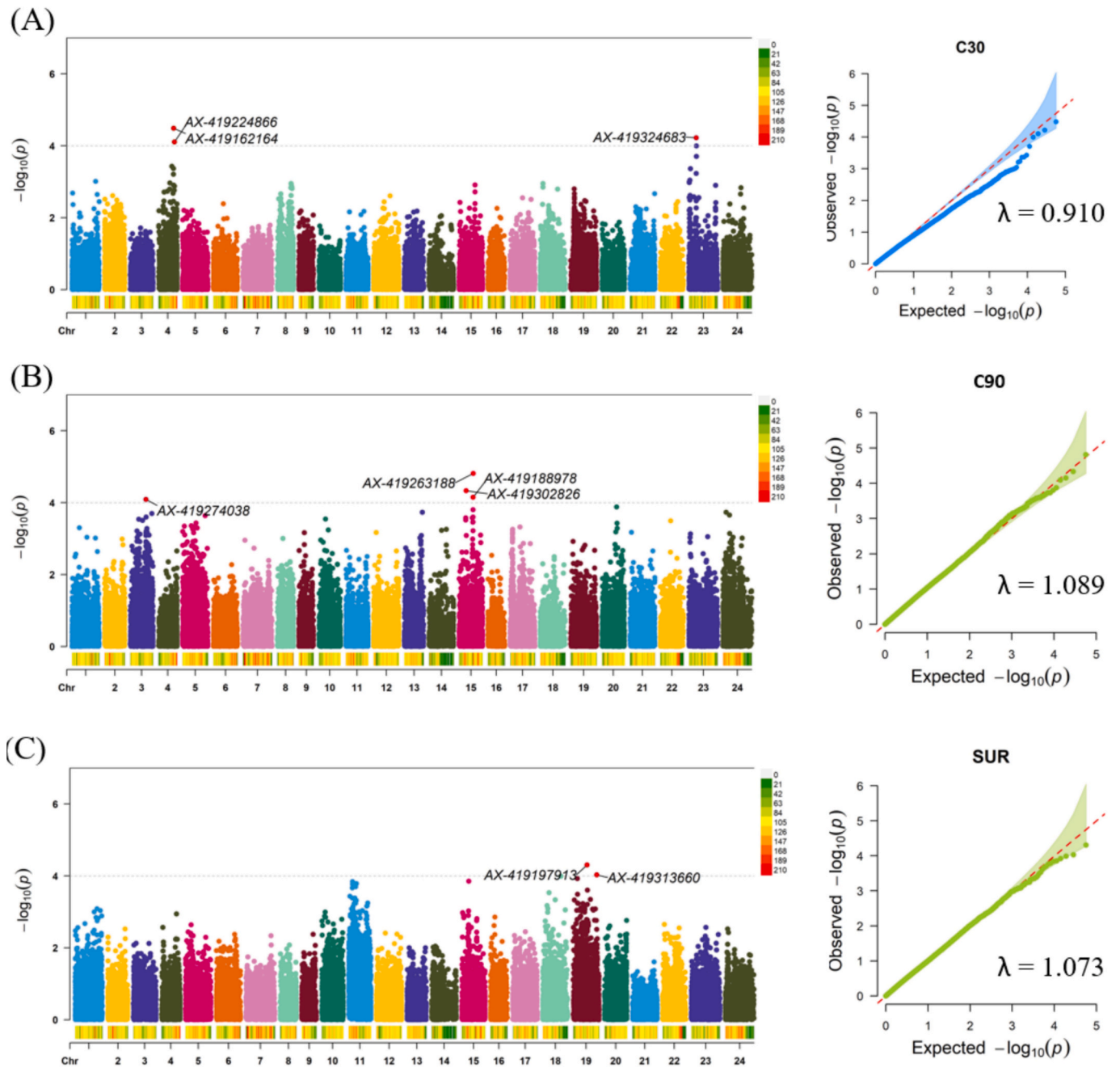

Fig. 4. Manhattan plots and QQ plots for the (A) cortisol level at 30 min, (B) cortisol level at 1 h (C) survival (D) DPC_date, and (E) DPC_time of the olive flounder. The solid black lines indicate the genome-wide significance threshold, and the dashed lines indicate the suggestive thresholds. SNPs exceeding the genome-wide cutoff are marked with red dots, while those above the suggestive cut-off are marked with green. Lambda (λ) values in the QQ plots denote the genomic inflation factors for the GWAS. (For interpretation of the references to color in this figure legend, the reader is referred to the web version of this article.)

3.6. SNP effects on cortisol levels and fish survival

Significant correlations were observed between fish genotypes and phenotypes, with several significant SNPs explaining up to 7 % of the phenotypic variance (Table 3). These correlations suggest that the SNPs play potential roles in cortisol regulation under acute high-temperature stress. Notably, when cortisol levels and sex were considered as fixed effects, SNPs that appeared to influence fish survival were identified. Nine candidate SNPs showed highly significant associations with DPC_time, DPC_date, and SUR (Supplementary Fig. 2), while six showed significant associations with cortisol level, with the significance level surpassing the suggestive significance threshold. Among the six SNPs, three were associated with cortisol level at the C30 and three at C90 (Table 3). Overall, among the 34 significant SNPs associated with C30, C90, DPC_time, DPC_date, and SUR, gene annotation analysis revealed that 2 SNPs were located in exons, 14 in introns, and 18 SNPs in intergenic regions (Supplementary Table 2).

3.7. Functional enrichment analysis of candidate genes using DAVID

The analysis of GWAS results using based on DAVID led to the identification of 20 candidate genes associated with the significant SNPs. The functional annotation of these genes based on three functional categories: biological processes, cellular components, and molecular

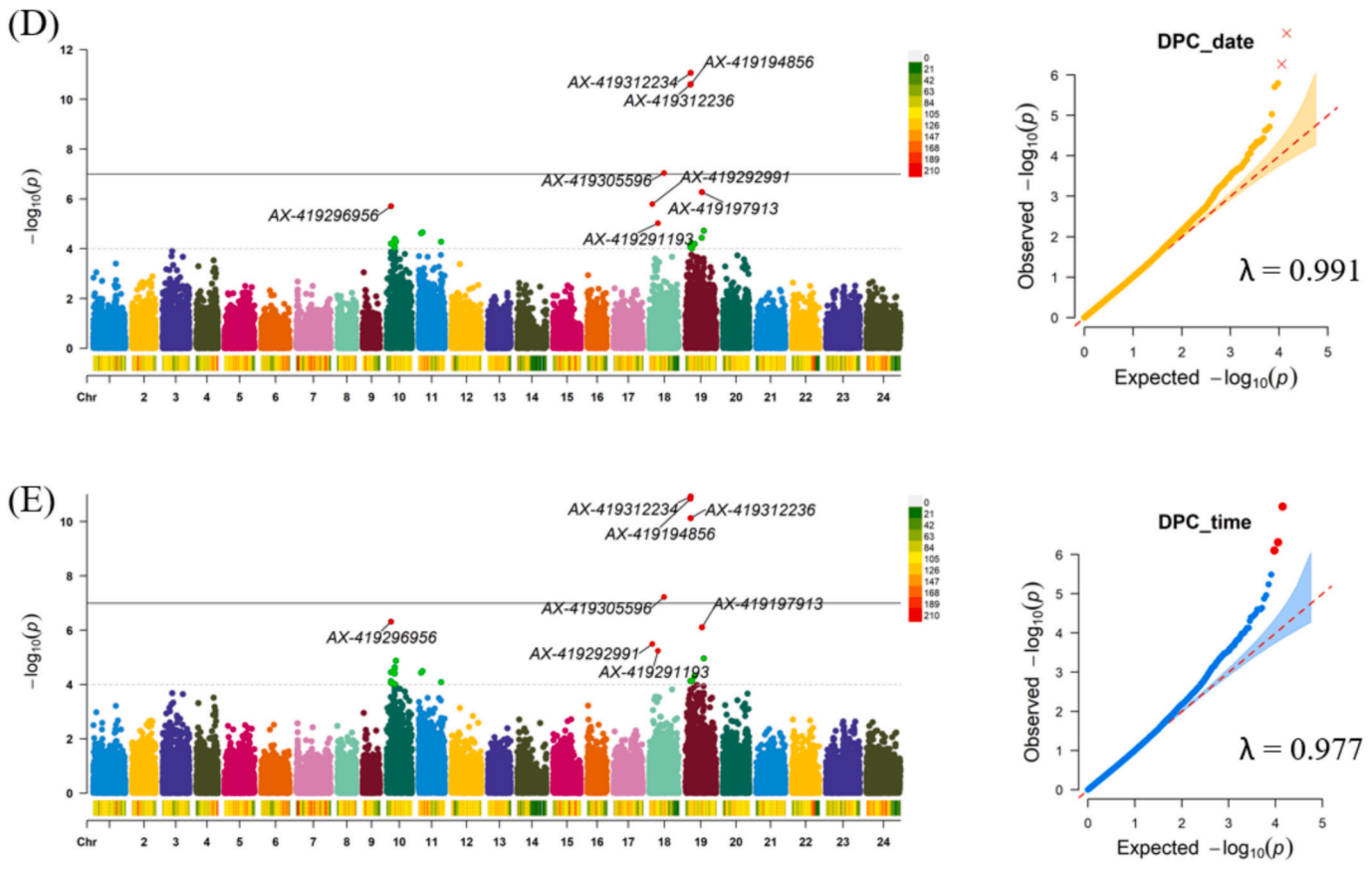

Fig. 4. (*continued*).

Table 2
Genotypic variance (V(G)), environmental variance (V(e)), phenotypic variance (Vp), and heritability estimates (V(G)/Vp) for five phenotypes.

Phenotype	V(G)	V(e)	V(p)	Heritability (V(G)/V(p))
C30	0.000046	45.71	45.71	0.000001
C90	2.153	54.31	56.46	0.038
SUR	0.0282	0.08	0.11	0.252
DPC_date	1.352	1.63	2.99	0.454
DPC_time	851.78	1015.69	1867.47	0.458

functions revealed the enrichment of genes associated with six biological process terms, three molecular function terms, and two cellular component terms. These enrichment patterns were further visualized using a bubble plot (Supplementary Fig. 3), which showed that all the identified genes were directly or indirectly associated with cellular and biological processes, molecular functions, and binding activities related to thermal homeostasis.

4. Discussion

Environmental stressors, including high temperature, hypoxia, and low salinity, significantly affect the aquaculture industry as they induce behavioral and structural changes in aquatic organisms, leading to significant production losses. To counter these challenges, fish activate endocrine pathways and defense mechanisms that help maintain homeostasis [21]. Among the abovementioned stressors, heat stress is particularly concerning owing to its association with an elevated mortality rate [22]. Acute high-temperature-related mortality can be triggered by multiple factors, including transportation stress, reduced dissolved oxygen levels, suboptimal tank design, and inadequate water flow. Consequently, developing stress-tolerant aquaculture species is crucial for ensuring sustainable production.

The current study addressed this challenge by employing GWAS to

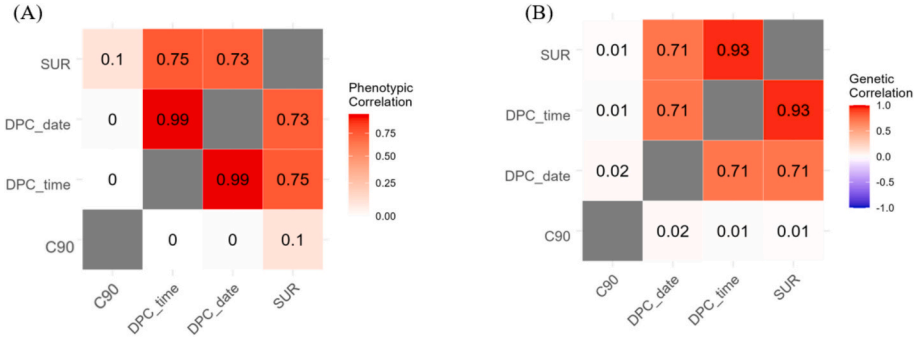

Fig. 5. Heat map of (A) phenotypic correlation (B) genetic correlation and across four traits.

Table 3
Significant SNPs and associated candidate genes identified by GWAS for stress-related and thermal tolerance traits in olive flounder.

Chr	SNP ID	Position (bp)	A1	A2	FrEq. (A2)	P-value	Significance	VarP (%)	Associated gene	Associated trait
19	AX-419312234	4,330,372	C	T	0.614361702	8.69E-12	Genome-wide	7 %	Myosin heavy chain, fast skeletal muscle-like, transcript variant X2 (***myhc***)	DPC_date and DPC_time
19	AX-419312236	4,344,315	G	A	0.635869565	2.48E-11	Genome-wide	6.7 %	NLR family CARD domain containing 5 (***nlrc5***)	DPC_date and DPC_time
19	AX-419194856	4,248,358	A	C	0.542553191	2.58E-11	Genome-wide	6.7 %	HYDIN, axonemal central pair apparatus protein (***hydin***)	DPC_date and DPC_time
18	AX-419305596	12,631,578	G	A	0.554521277	9.23E-08	Genome-wide	4.5 %	Glucose-fructose oxidoreductase domain-containing protein 1 (***gfod1***)	DPC_date and DPC_time
19	AX-419197913	14,012,485	T	C	0.543882979	5.37E-07	Genome-wide	4 %	S-phase cyclin A associated protein in the ER (***scaper***)	DPC_date, DPC_time and SUR
18	AX-419292991	2,390,583	G	A	0.634308511	1.61E-06	Suggestive	3.6 %	Catenin delta-2-like, transcript variant X4 (***ctnnd2***)	DPC_date and DPC_time
10	AX-419296956	3,777,074	C	T	0.63368984	1.99E-06	Suggestive	3.6 %	RNA binding protein fox-1 homolog 2-like (***rbfox2***)	DPC_date and DPC_time
18	AX-419291193	7,299,387	A	G	0.537533512	9.39E-06	Suggestive	3.1 %	Chromosome unknown C3orf58 homolog, transcript variant X2 (***cunh3orf58***)	DPC_date and DPC_time
15	AX-419263188	14,331,018	T	C	0.66	1.55E-05	Suggestive	2.9 %	Ephrin B2, transcript variant X2 (***efnb2***)	C90
19	AX-419195929	15,640,134	G	A	0.5625	1.91E-05	Suggestive	2.9	Cadherin-related family member 5-like (***cdhr5***)	DPC_date and DPC_time
11	AX-419250528	3,479,233	A	C	0.865691489	2.20E-05	Suggestive	2.9 %	TSC22 domain family protein 2-like (***tsc22d2***)	DPC_date and DPC_time
11	AX-419178439	2,265,643	A	G	0.825333333	2.40E-05	Suggestive	2.9 %	Ribosomal protein S15 (***rps15***)	DPC_date and DPC_time
4	AX-419162164	15,473,804	C	T	0.77393617	3.28E-05	Suggestive	3.3 %	Urotensin-2 receptor-like (***uts2r***)	C30
19	AX-419312138	13,866,568	C	T	0.613031915	3.65E-05	Suggestive	2.7 %	Talin 2, transcript variant X6 (***tln2***)	DPC_date and DPC_time
10	AX-419275573	7,107,648	T	C	0.545576408	4.05E-05	Suggestive	2.7 %	PET100 homolog (***pet100***)	DPC_date and DPC_time
10	AX-419273595	7,105,576	A	G	0.545212766	4.50E-05	Suggestive	2.7 %	PET100 homolog (***pet100***)	DPC_date and DPC_time
10	AX-419178488	7,108,662	G	A	0.545212766	4.50E-05	Suggestive	2.7 %	PET100 homolog (***pet100***)	DPC_date and DPC_time
10	AX-419248002	7,101,264	G	A	0.545212766	4.50E-05	Suggestive	2.7 %	PET100 homolog (***pet100***)	DPC_date and DPC_time
15	AX-419302826	7,129,383	A	G	0.647453083	4.67E-05	Suggestive	2.6 %	Peptidyl-prolyl cis-trans isomerase-like (***ppil***)	C90
11	AX-419303472	19,397,451	T	C	0.825797872	5.31E-05	Suggestive	2.6 %	Dystrobrevin alpha-like (***dtna***)	DPC_date and DPC_time
19	AX-419197121	5,075,058	T	C	0.660857909	6.04E-05	Suggestive	2.6	Guanine nucleotide-binding protein G(o) subunit alpha (***gnao1***)	DPC_date and DPC_time
23	AX-419324683	7,360,126	T	C	0.779255319	6.04E-05	Suggestive	3 %	DNA, contains MHC class Ia chain, clone: BAC-55I6 (***mhc***)	C30
10	AX-419288429	3,755,655	A	G	0.544	6.27E-05	Suggestive	2.6 %	RNA binding protein fox-1 homolog 2-like (***rbfox2***)	DPC_date and DPC_time
19	AX-419312717	7,822,959	T	C	0.546542553	6.42E-05	Suggestive	2.6 %	Monocarboxylate transporter 13-like, transcript variant X3 (***mcts***)	DPC_date and DPC_time
15	AX-419188978	14,315,040	T	G	0.575880759	7.11E-05	Suggestive	2.5 %	Ephrin B2, transcript variant X2 (***efnb2***)	C90
10	AX-419295423	3,805,009	T	C	0.568918919	7.51E-05	Suggestive	2.5 %	Uncharacterized LOC109646336 (LOC109646336)	DPC_date and DPC_time
4	AX-419224866	16,199,792	T	C	0.740691489	7.84E-05	Suggestive	3 %	Glucagon like peptide 2 receptor (***glp2r***)	C30
10	AX-419248000	7,100,487	T	C	0.636968085	8.60E-05	Suggestive	2.5 %	Myosin heavy chain, fast skeletal muscle (***myhc***)	DPC_date and DPC_time
19	AX-419194853	4,230,401	A	G	0.751329787	8.68E-05	Suggestive	2.5 %	HYDIN, axonemal central pair apparatus protein (***hydin***)	DPC_date and DPC_time
10	AX-177849800	3,791,404	A	C	0.534574468	8.69E-05	Suggestive	2.5 %	CD9 antigen-like, transcript variant X2 (***cd9***)	DPC_date and DPC_time
10	AX-419273564	6,865,375	A	G	0.505319149	9.06E-05	Suggestive	2.5 %	Collagen alpha-1(XI) chain, transcript variant X3 (***col11a1***)	DPC_date and DPC_time
19	AX-419313660	23,974,713	C	T	0.506648936	9.40E-05	Suggestive	2.5 %	REST corepressor 3 (***rcor3***)	SUR
19	AX-419197179	5,704,736	C	A	0.646276596	9.61E-05	Suggestive	2.4 %	USP6 N-terminal-like protein, transcript variant X2 (***usp6n***)	DPC_date and DPC_time
10	AX-419275564	7,065,718	T	C	0.56097561	9.63E-05	Suggestive	2.5 %	Myosin heavy chain, fast skeletal muscle (***myhc***)	DPC_date and DPC_time

identify SNPs that are associated with cortisol level, a key marker of acute and chronic high-temperature stress in olive flounder, and provide a foundation for understanding the genetic mechanisms underlying both acute and chronic stress responses. Although previous studies have examined the physiological responses of olive flounder to thermal stress [23], the genetic factors underlying acute stress responses remain poorly understood. Further, we examined chronic thermal tolerance in the same individuals subjected to acute thermal stress with the expectation

that combining the results would provide a more comprehensive understanding of the resilience and adaptability of olive flounders to high temperatures.

Olive flounders exhibit broad-range temperature tolerance considering their diverse habitats, with wild populations surviving in waters below 9 °C in winter and above 27 °C in summer. However, their optimal rearing temperature in South Korea ranges from 19 to 21 °C [24], and despite their adaptability, sudden temperature fluctuations can induce acute stress, highlighting the need to clarify the genetic mechanisms underlying their responses to such conditions. Moreover, prolonged exposure to elevated temperatures, especially as global warming drives environmental temperatures beyond optimal ranges, induces chronic stress. Therefore, we hypothesized that similar to Atlantic salmon, olive flounder populations harbor additive genetic variations that contribute to both acute and chronic high-temperature stress tolerance [25].

The heritability of chronic high-temperature tolerance in olive flounder is estimated to be 0.29 [13]. Similarly, Ma et al. reported heat stress tolerance heritabilities in the range 0.019 to 0.239 for four turbot stocks from England, France, Denmark, and Norway [26]. To the best of our knowledge however, the present study is the first to investigate the heritability of acute high-temperature stress in olive flounder. Based on a 1-h exposure assessment, C90 heritability was estimated to be 0.038, which was low; however, chronic high-temperature stress traits showed moderate heritability, with the values at 0.454, 0.458, and 0.252 for DPC_date, DPC_time, and SUR, respectively. These findings indicated that selective breeding could potentially enhance high-temperature stress tolerance.

QC filtering yielded 57,638 SNPs across 24 chromosomes from 376 individuals. Further, PCA and cross-validation identified three distinct populations within the experimental group and the PCA plot revealed shared genetic characteristics among individuals in these clusters, suggesting minimal genetic differences based on ancestral backgrounds. These shared characteristics possibly reflect the genetic relatedness captured by the analysis [27]. Additionally, the GRM heat map corroborated these findings by visually illustrating three major population groups.

Positive phenotypic correlations were observed among all traits, along with moderate correlations between the genotypic and phenotypic traits. These positive genetic correlations may benefit breeding programs by enabling the simultaneous improvement of multiple traits [28]. Notably, C90 showed lower positive correlations with all other traits, including SUR. This observation possibly suggesting that cortisol level plays a complex role in acute stress response and could be improved concurrently with chronic thermal tolerance traits.

GWAS effectively identified SNPs associated with specific traits. Several of these markers were located within or near previously reported thermal stress response genes, while a few others were located in regions containing unknown genes or regulatory elements, potentially indicating novel genetic mechanisms underlying the complexity of heat stress response. Building on a previous study, wherein thermal stress response genes were categorized into four groups (metabolic, neural/neuroendocrine, molecular/cellular, and physiological/behavioral) [13], we identified highly significant SNPs associated with C30 and C90 post-exposure. These findings highlighted the diverse physiological processes involved in thermal stress response, including energy production and utilization, nervous system regulation, cellular repair mechanisms, and behavioral adaptations.

Urotensin-2 receptor (UTS2R), primarily expressed in vascular and cardiac tissues, functions as a receptor of vasoactive peptide urotensin-II, and its upregulation influences heart rate and blood pressure regulation [29]. During acute temperature elevation, UTS2R may help modulate cardiovascular responses by inducing blood vessel constriction or dilation, and thus, maintain circulatory homeostasis under stress. Additionally, studies have shown that UTS2R is implicated in the regulation of stress-induced lymphocyte DNA damage and oxidative changes in mammals, suggesting a protective function against stress-induced cellular damage [29].

Further, MHC class Ia chain, a critical component of the immune system, is responsible for presenting antigens to cytotoxic T cells. While acute heat stress can impair immune function, making fish more susceptible to infections, MHC class Ia molecules help to maintain immune competence during thermal stress by enhancing antigen presentation and promoting T-cell activation [30].

EFNB2, a member of the ephrin signaling family, is essential for mediating cell communication and development. Specifically, ephrin signaling facilitates multiple stress-adaptive processes such as cell survival, angiogenesis, tissue repair, and inflammation regulation [31]. Our findings indicate that EFNB2 plays a crucial role in the recovery and adaptation of olive flounder to high-temperature stress.

GLP2R, predominantly expressed in mammalian gut tissues, promotes intestinal growth and nutrient uptake [32], and its expression in fish gut tissues during stress suggests that it is implicated in post-stress recovery rather than in immediate response. It has also been reported that after acute thermal stress, GLP2R likely contributes to maintaining gut health by enhancing nutrient absorption, promoting tissue regeneration, and restoring energy metabolism [33], indicating that it plays an important role in long-term recovery and stress resilience.

PPIase-like genes represent an emerging area of research in fish stress resilience. While their specific roles in acute thermal stress response remain unclear, their known functions in protein folding, signaling regulation, and cellular protection suggest their involvement in complex stress response networks. Although the exact mechanisms are unknown, it is possible that *PPIase-like* genes influence cortisol regulation by modulating the signaling pathways involved in cortisol synthesis or release and by interacting with cortisol-binding proteins [34]. In mammals, mutations in these genes are associated with neurodegenerative conditions, such as pontocerebellar hypoplasia with microcephaly (PCHM) [35], implying that they play important roles in neuronal development and function. However, further research is necessary to elucidate their specific roles in stress response in olive flounder.

Acute high-temperature stress triggers cortisol release in fish, and this stress-response mechanism is highly conserved across vertebrates. Elevated cortisol levels can compromise fish health by causing immunosuppression, growth reduction, and increased disease susceptibility. However, genetic variations may modulate stress resilience by altering the magnitude and duration of cortisol release. Further, the identification of significant stress resilience-associated SNPs advances our understanding of the genomic basis for enhanced stress tolerance in olive flounder, and these SNPs represent promising targets for selective breeding programs.

In addition to examining the genes involved in acute high-temperature stress response, we investigated the genetic basis of chronic high-temperature stress tolerance. Thus, we identified significant SNPs associated with chronic high-temperature stress tolerance. Several of these SNPs were found to be located within or close to genes that have been implicated in heat shock response, antioxidant defense, and DNA repair [13]. Notably, the most significant SNP was located within the *MyHC* gene, which encodes the myosin heavy chain, a key protein involved in muscle contraction. This observation suggested that MyHC plays a key role in maintaining motor function and survival during thermal stress, particularly because swimming patterns are affected by increasing temperatures. Previous studies have also reported upregulated *MyHC* expression in Japanese rice fish exposed to high temperatures, particularly in the lower skeletal muscle [36,37].

The second most significant SNP was located in the gene region of *NLRC5*, a well-known immune regulatory gene that directly influences innate immune response. Specifically, *NLRC5* interacts with IFN-γ to stimulate downstream pro-inflammatory response genes, such as *TNF-α*, *IL-6*, and *IL-1β* [38], suggesting that it plays a crucial role in maintaining immune function and combating infection under chronic high-temperature stress.

The third most significant SNP was located within the *HYDIN* gene,

which is associated with sensory perception and has been previously associated with pain sensitivity under heat stress conditions possibly because HYDIN plays a key role in controlling the movement of cilia, i.e., hair-like structures within the brain that regulate cerebrospinal fluid flow [39]. The disruption of ciliary function may impair sensory perception and contribute to the adverse effects of heat stress.

Further, 26 additional significant SNPs associated with genes involved in diverse functions were identified, indicating that a complex genetic architecture underlies thermal tolerance in olive flounder. For instance, one SNP showed association with *GOD1*, which is involved in carbohydrate metabolism [40]. Notably, carbohydrates serve as a primary energy source given that they can be readily be converted into ATP, which fuels various metabolic processes. Under chronic high-temperature stress, energy demands increase significantly owing to factors such as protein refolding for heat damage repair and decreased reliance on fat utilization [41]. Consequently, accelerated carbohydrate metabolism is required to generate the necessary energy surplus. Therefore, the observed association between an SNP and *GOD1* suggest that *GOD1* expression is likely upregulated under thermal stress to enhance carbohydrate metabolism and meet the elevated energy requirements of stressed fish.

GNAO1, previously identified in mice, encodes a protein that is involved in neuroendocrine functions, and reportedly, it regulates calcium-dependent neuronal signaling, growth, and cytoskeletal remodeling [42], implying that its role in neural developmental processes may be critical for coordinating physiological responses to thermal stress. In olive flounder, *GNAO1* may also play a key role in integrating physiological and behavioral responses to chronic thermal stress, possibly by influencing the release of stress hormones or modulating neuronal activity in response to temperature changes.

CTNND2 has emerged as a potential candidate gene implicated in response to elevated water temperatures, possibly via the mitigation of the effects of hypoxia, which is common in warmer rearing environments. Increased metabolic demands in fish due to elevated temperatures often lead to increased ventilation rates as hypoxia develops. Studies have also suggest that hypoxia-inducible factor (HIF) directly upregulates *CTNND2* expression, resulting in the production of δ-catenin [43], which acts as a downstream target of HIF-1α and may help regulate cellular response to hypoxia. Further, *RBFOX2* has been identified as a hypoxia-inducible gene [44], and together with the abovementioned, these genes may be crucial for maintaining oxygen homeostasis and ensuring survival in oxygen-depleted environments under thermal stress.

CDHR5, a gene that is highly expressed in the epithelial cell microvilli of the intestine and kidney, plays a crucial role in nutrient transport and absorption [45]. During thermal stress, elevated metabolic rates in fish necessitate increased nutrient uptake and efficient digestion. Under these conditions, enhanced *CDHR5* expression may boost nutrient and ion absorption through microvilli to meet heightened metabolic demands and support survival.

A significant SNP was identified within the *TSC22* gene, which plays a vital role in regulating tissue osmotic pressure, especially with increasing water temperatures [46]. Maintaining proper tissue osmotic balance is critical for fish survival, and midwater fish are particularly susceptible to disruptions in this equilibrium. It has also been shown that elevated temperatures reduce the activity of Na^+/K^+-ATPase, an essential enzyme that maintains osmotic balance in gill tissues [47], ultimately disrupting osmotic equilibrium and posing a significant threat to fish survival. Therefore, *TSC22* may be crucial for maintaining osmotic balance and preventing cellular damage under thermal stress. Several other genes with significant SNPs that potentially affect thermal resistance were identified, including *TLN2*, *PET100*, *DTNA*, *MCTs*, *RCOR3*, and *USP6N*, all of which have been implicated in various physiological functions [48–54]. Interestingly, *RPS15* plays a role in immune response regulation [48].

Overall, these findings highlight the complex genetic architecture underlying thermal stress resistance in olive flounder, involving genes that regulate diverse physiological processes, such as oxygen homeostasis, nutrient absorption, osmotic balance, and immune response.

To comprehensively clarify the pathways involved in thermal stress response in olive flounder, our analysis using DAVID focused on three main functional categories, biological processes, cellular components, and molecular functions. Complementary annotations based on InterPro, UP_KW_Domain, and UP_SEQ_Feature provided additional insights into protein functions at the molecular level; sequence features within biological, molecular, and cellular contexts; and clarified the interactions among the 20 candidate genes identified in this study. This multifaceted approach enhanced our understanding of the functional roles of these genes in thermal stress response. Previous studies have shown that biological processes and cellular components play critical roles in response to high-temperature stress [55], indicating that organisms must adapt to extreme temperatures to maintain cellular homeostasis and reduce stress levels [56]. Notably, cell–cell adhesion exhibited the highest statistical significance, suggesting a strong association between thermal tolerance and stress resilience. Further, it played a crucial role in maintaining tissue integrity and cellular communication under environmental stress conditions [57]. Therefore, enhanced cell–cell adhesion possibly contributed to thermal tolerance and stress resilience by stabilizing cellular structures, reducing stress-induced damage, and facilitating coordinated stress response mechanisms. For example, cellular stress response pathways, such as the heat shock response pathway, are activated to protect cells from high temperature-induced damage. Although rising temperatures may initially enhance the activity of certain molecular functions, sustained exposure can eventually lead to dramatic inhibition [58], and thus, disrupt molecular pathways by altering DNA, RNA, and protein synthesis [59], and ultimately impairing cellular function and viability.

In conclusion, this study, to the best of our knowledge, is the first to investigate both acute and chronic high-temperature stress resistance in olive flounder using the GWAS approach. Specifically, we identified 34 significant SNPs associated with thermal stress resistance. These SNPs were also associated with various genes that directly or indirectly mediate thermal tolerance and help maintain physiological homeostasis during high-temperature exposure. Notably, *MyHC*, *NLRC5*, *HYDIN*, and *GOD1*, which have been previously implicated in thermal tolerance in other species, were identified in this study, further supporting their importance in stress response. DAVID analysis also confirmed the existence of associations between these candidate genes and thermal stress resistance. Moreover, the moderate heritability of stress-induced cortisol levels and the high heritability of fish survival under chronic stress conditions underscored the potential of these traits for improving olive flounder aquaculture sustainability via MAS and genomic selection, i.e., by incorporating these markers into breeding programs, the resilience of olive flounder to thermal stress may be enhanced, thereby improving their sustainability and profitability amid climate change and other environmental challenges. The findings of this study also provide valuable insights that may enhance understanding regarding the mechanisms of thermal stress response in other fish species, contributing to a broader understanding of stress responses in vertebrates.

CRediT authorship contribution statement

H.A.C.R. Hanchapola: Writing – original draft, Visualization, Validation, Software, Investigation, Formal analysis, Conceptualization. **Po Gong:** Visualization, Methodology, Investigation, Data curation. **Gaeun Kim:** Visualization, Validation, Methodology, Investigation, Formal analysis, Data curation. **D.S. Liyanage:** Writing – review & editing, Visualization, Validation, Software, Methodology, Investigation, Formal analysis, Data curation. **W.K.M. Omeka:** Writing – review & editing, Validation, Methodology, Investigation. **Jeongeun Kim:** Methodology, Investigation. **Y.K. Kodagoda:** Methodology, Investigation. **M.A.H. Dilshan:** Methodology, Investigation. **D.C.G. Rodrigo:**

Methodology, Investigation. **G.A.N. Piyumika Ganepola:** Methodology, Investigation. **Cecile Massault:** Writing – review & editing, Validation, Supervision, Software. **Dean R. Jerry:** Writing – review & editing, Validation, Supervision, Software. **Jihun Lee:** Validation, Supervision, Software, Investigation. **Jehee Lee:** Writing – review & editing, Validation, Supervision, Resources, Project administration, Funding acquisition, Data curation.

Declaration of competing interest

The authors declare that they have no known competing financial interests or personal relationships that could have appeared to influence the work reported in this paper.

Acknowledgments

This work was supported by the 2025 National University Development Project grant of Jeju National University funded by the Ministry of Education.

Appendix A. Supplementary data

Supplementary data to this article can be found online at https://doi.org/10.1016/j.ygeno.2025.111124.

Data availability

Data will be made available on request.

References

[1] R. Guenard, The State of World Fisheries and Aquaculture 2020, FAO, 2020, https://doi.org/10.4060/ca9229en.
[2] M. Vermeer, S. Rahmstorf, Global sea level linked to global temperature, Proc. Natl. Acad. Sci. 106 (2009) 21527–21532, https://doi.org/10.1073/pnas.0907765106.
[3] J.W. Hur, H.K. Lim, Y.J. Chang, Effects of repetitive temperature changes on the stress response and growth of olive flounder, *Paralichthys olivaceus*, J. Appl. Anim. Res. 33 (2008) 49–54, https://doi.org/10.1080/09712119.2008.9706895.
[4] A. Madaro, R.E. Olsen, T.S. Kristiansen, L.O.E. Ebbesson, T.O. Nilsen, G. Flik, M. Gorissen, Stress in Atlantic salmon: response to unpredictable chronic stress, J. Exp. Biol. 218 (2015) 2538–2550, https://doi.org/10.1242/jeb.120535.
[5] E.H. Ignatz, M.S. Allen, J.R. Hall, R.M. Sandrelli, M.D. Fast, G.M.L. Perry, M. L. Rise, A.K. Gamperl, Application of genomic tools to study and potentially improve the upper thermal tolerance of farmed Atlantic salmon (*Salmo salar*), BMC Genomics 26 (2025) 294, https://doi.org/10.1186/s12864-025-11482-4.
[6] B. Sadoul, S. Alfonso, X. Cousin, P. Prunet, M.-L. Bégout, I. Leguen, Global assessment of the response to chronic stress in European sea bass, Aquaculture 544 (2021) 737072, https://doi.org/10.1016/j.aquaculture.2021.737072.
[7] J. Murtha, Characterization of the heat shock response in mature zebrafish (*Danio rerio*), Exp. Gerontol. 38 (2003) 683–691, https://doi.org/10.1016/S0531-5565(03)00067-6.
[8] K. Park, E.J. Han, G. Ahn, I.-S. Kwak, Effects of combined stressors to cadmium and high temperature on antioxidant defense, apoptotic cell death, and DNA methylation in zebrafish (*Danio rerio*) embryos, Sci. Total Environ. 716 (2020) 137130, https://doi.org/10.1016/j.scitotenv.2020.137130.
[9] J.F. López-Olmeda, F.J. Sánchez-Vázquez, Thermal biology of zebrafish (*Danio rerio*), J. Therm. Biol. 36 (2011) 91–104, https://doi.org/10.1016/j.jtherbio.2010.12.005.
[10] B.A. Barton, Stress in fishes: a diversity of responses with particular reference to changes in circulating corticosteroids, Integr. Comp. Biol. 42 (2002) 517–525, https://doi.org/10.1093/icb/42.3.517.
[11] W.K.M. Omeka, D.S. Liyanage, S. Lee, C. Lim, H. Yang, W.M.G. Sandamalika, H.M. V. Udayantha, G. Kim, S. Ganeshalingam, T. Jeong, S.-R. Oh, S.-H. Won, H.-B. Koh, M.-K. Kim, D.B. Jones, C. Massault, D.R. Jerry, J. Lee, Genome-wide association study (GWAS) of growth traits in olive flounder (*Paralichthys olivaceus*), Aquaculture 555 (2022) 738257, https://doi.org/10.1016/j.aquaculture.2022.738257.
[12] D.S. Liyanage, S. Lee, H. Yang, C. Lim, W.K.M. Omeka, W.M.G. Sandamalika, H.M. V. Udayantha, G. Kim, S. Ganeshalingam, T. Jeong, S.-R. Oh, S.-H. Won, H.-B. Koh, M.-K. Kim, D.B. Jones, C. Massault, D.R. Jerry, J. Lee, Genome-wide association study of VHSV-resistance trait in *Paralichthys olivaceus*, Fish Shellfish Immunol. 124 (2022) 391–400, https://doi.org/10.1016/j.fsi.2022.04.021.
[13] H.M.V. Udayantha, S. Lee, D.S. Liyanage, C. Lim, T. Jeong, W.K.M. Omeka, H. Yang, G. Kim, J. Kim, J. Lee, K. Nadarajapillai, S. Ganeshalingam, C.-U. Park, J. Lee, S.-R. Oh, P. Gong, Y. Jang, J. Hyun, A. Park, H.-B. Koh, M.-K. Kim, D. B. Jones, C. Massault, D.R. Jerry, J. Lee, Identification of candidate variants and genes associated with temperature tolerance in olive flounders by genome-wide association study (GWAS), Aquaculture 576 (2023) 739858, https://doi.org/10.1016/j.aquaculture.2023.739858.
[14] Y.K. Kodagoda, G. Kim, D.S. Liyanage, W.K.M. Omeka, C. Park, J. Kim, J.H. Lee, H. A.C.R. Hanchapola, M.A.H. Dilshan, D.C.G. Rodrigo, D.B. Jones, C. Massault, D. R. Jerry, J. Lee, Genome-wide association mapping of scuticociliatosis resistance in a vaccinated population of olive flounder (*Paralichthys olivaceus*), Fish Shellfish Immunol. 162 (2025) 110339, https://doi.org/10.1016/j.fsi.2025.110339.
[15] C.C. Chang, C.C. Chow, L.C. Tellier, S. Vattikuti, S.M. Purcell, J.J. Lee, Second-generation PLINK: rising to the challenge of larger and richer datasets, Gigascience 4 (2015) 7, https://doi.org/10.1186/s13742-015-0047-8.
[16] L. Yin, H. Zhang, Z. Tang, J. Xu, D. Yin, Z. Zhang, X. Yuan, M. Zhu, S. Zhao, X. Li, X. Liu, rMVP: a memory-efficient, visualization-enhanced, and parallel-accelerated tool for genome-wide association study, genomics, Proteomics Bioinform. 19 (2021) 619–628, https://doi.org/10.1016/j.gpb.2020.10.007.
[17] B.C. Epitope, Encyclopedia of Systems Biology, Springer New York, New York, NY, 2013, https://doi.org/10.1007/978-1-4419-9863-7.
[18] Y. Yang, L. Wu, X. Wu, B. Li, W. Huang, Z. Weng, Z. Lin, L. Song, Y. Guo, Z. Meng, X. Liu, J. Xia, Identification of candidate growth-related SNPs and genes using GWAS in Brown-marbled grouper (*Epinephelus fuscoguttatus*), Mar. Biotechnol. 22 (2020) 153–166, https://doi.org/10.1007/s10126-019-09940-8.
[19] A.B. Schmid, K. Adhikari, L.M. Ramirez-Aristeguieta, J.C. Chacón-Duque, G. Poletti, C. Gallo, F. Rothhammer, G. Bedoya, A. Ruiz-Linares, D.L. Bennett, Genetic components of human pain sensitivity: a protocol for a genome-wide association study of experimental pain in healthy volunteers, BMJ Open 9 (2019) 1–10, https://doi.org/10.1136/bmjopen-2018-025530.
[20] M.L. Aslam, R. Carraro, A.K. Sonesson, T. Meuwissen, C.S. Tsigenopoulos, G. Rigos, L. Bargelloni, K. Tzokas, Genetic variation, GWAS and accuracy of prediction for host resistance to Sparicotyle chrysophrii in farmed Gilthead Sea bream (*Sparus aurata*), Front. Genet. 11 (2020) 594770, https://doi.org/10.3389/fgene.2020.594770.
[21] S.E. Wendelaar Bonga, The stress response in fish, Physiol. Rev. 77 (1997) 591–625, https://doi.org/10.1152/physrev.1997.77.3.591.
[22] I. Belhadj Slimen, T. Najar, A. Ghram, M. Abdrrabba, Heat stress effects on livestock: molecular, cellular and metabolic aspects, a review, J. Anim. Physiol. Anim. Nutr. (Berl). 100 (2016) 401–412, https://doi.org/10.1111/jpn.12379.
[23] G.L. Bennett, E.J. Pollak, L.A. Kuehn, W.M. Snelling, Breeding: animals, in: N. K. Van Alfen (Ed.), Encycl. Agric. Food Syst, Elsevier, Oxford, 2014, pp. 173–186, https://doi.org/10.1016/B978-0-444-52512-3.00228-X.
[24] D.-H. Oh, S.-S. Kim, K.-W. Kim, K.-D. Kim, B.-J. Lee, H.-S. Han, J.-W. Kim, O. E. Okorie, S.C. Bai, K.-J. Lee, Optimum feeding rate for growing olive flounder (317 g) *Paralichthys olivaceus* fed practical extruded pellets at optimum water temperature (21-24°C), Korean, J. Fish. Aquat. Sci. 47 (2014) 399–405, https://doi.org/10.5657/KFAS.2014.0399.
[25] P.V. Debes, M.F. Solberg, I.H. Matre, L. Dyrhovden, K.A. Glover, Genetic variation for upper thermal tolerance diminishes within and between populations with increasing acclimation temperature in Atlantic salmon, Heredity (Edinb). 127 (2021) 455–466, https://doi.org/10.1038/s41437-021-00469-y.
[26] A. Ma, X. Wang, Z. Huang, Z. Liu, W. Cui, J. Qu, Estimation of genetic parameters for upper thermal tolerance and growth-related traits in turbot *Scophthalmus maximus* using the Bayesian method based on Gibbs sampling, Acta Oceanol. Sin. 37 (2018) 40–46, https://doi.org/10.1007/s13131-018-1185-5.
[27] R. Eid, C. Landès, A. Pernet, E. Benoît, P. Santagostini, A. El Ghaziri, J. Bourbeillon, DIVIS: a semantic DIstance to improve the VISualisation of heterogeneous phenotypic datasets, BioData Min. 15 (2022) 10, https://doi.org/10.1186/s13040-022-00293-y.
[28] S. Toghiani, Quantitative genetic application in the selection process for livestock production, in: Livest. Prod, InTech, 2012, https://doi.org/10.5772/51027.
[29] M. Yigit, O. Sogut, Ö. Tataroglu, A. Yamanoglu, E. Yigit, E.M. Guler, O.F. Ozer, A. Kocyigit, Oxidative/antioxidative status, lymphocyte DNA damage, and urotensin-2 receptor level in patients with migraine attacks, Neuropsychiatr. Dis. Treat. 14 (2018) 367–374, https://doi.org/10.2147/NDT.S156710.
[30] T. van Hall, C.C. Oliveira, S.A. Joosten, T.H.M. Ottenhoff, The other Janus face of Qa-1 and HLA-E: diverse peptide repertoires in times of stress, Microbes Infect. 12 (2010) 910–918, https://doi.org/10.1016/j.micinf.2010.07.011.
[31] Q. Zhang, J. Li, F. Liu, J. Hu, F. Liu, J. Zou, X. Wang, Ephrin B2 (EFNB2) potentially protects against intervertebral disc degeneration through inhibiting nucleus pulposus cell apoptosis, Arch. Biochem. Biophys. 756 (2024) 109990, https://doi.org/10.1016/j.abb.2024.109990.
[32] J. Bahrami, C. Longuet, L.L. Baggio, K. Li, D.J. Drucker, Glucagon-like Peptide-2 receptor modulates islet adaptation to metabolic stress in the Ob/Ob mouse, Gastroenterology 139 (2010) 857–868, https://doi.org/10.1053/j.gastro.2010.05.006.
[33] M. Conde-Sieira, M. Chivite, J.M. Míguez, J.L. Soengas, Stress effects on the mechanisms regulating appetite in teleost fish, Front. Endocrinol. (Lausanne) 9 (2018) 631, https://doi.org/10.3389/fendo.2018.00631.
[34] N.M. Galigniana, L.T. Ballmer, J. Toneatto, A.G. Erlejman, M. Lagadari, M. D. Galigniana, Regulation of the glucocorticoid response to stress-related disorders by the Hsp90-binding immunophilin FKBP51, J. Neurochem. 122 (2012) 4–18, https://doi.org/10.1111/j.1471-4159.2012.07775.x.
[35] G. Chai, A. Webb, C. Li, D. Antaki, S. Lee, M.W. Breuss, N. Lang, V. Stanley, P. Anzenberg, X. Yang, T. Marshall, P. Gaffney, K.J. Wierenga, B.H.-Y. Chung, M. H.-Y. Tsang, L.S. Pais, A.K. Lovgren, G.E. VanNoy, H.L. Rehm, G. Mirzaa, E. Leon, J. Diaz, A. Neumann, A.P. Kalverda, I.W. Manfield, D.A. Parry, C.V. Logan, C. A. Johnson, D.T. Bonthron, E.M.A. Valleley, M.Y. Issa, S.F. Abdel-Ghafar, M. S. Abdel-Hamid, P. Jennings, M.S. Zaki, E. Sheridan, J.G. Gleeson, Mutations in

Spliceosomal genes PPIL1 and PRP17 cause neurodegenerative pontocerebellar hypoplasia with microcephaly, Neuron 109 (2021) 241–256.e9, https://doi.org/10.1016/j.neuron.2020.10.035.
[36] C.-S. Liang, A. Kobiyama, A. Shimizu, T. Sasaki, S. Asakawa, N. Shimizu, S. Watabe, Fast skeletal muscle myosin heavy chain gene cluster of medaka *Oryzias latipes* enrolled in temperature adaptation, Physiol. Genomics 29 (2007) 201–214, https://doi.org/10.1152/physiolgenomics.00078.2006.
[37] A. Weiss, D. McDonough, B. Wertman, L. Acakpo-Satchivi, K. Montgomery, R. Kucherlapati, L. Leinwand, K. Krauter, Organization of human and mouse skeletal myosin heavy chain gene clusters is highly conserved, Proc. Natl. Acad. Sci. USA 96 (1999) 2958–2963, https://doi.org/10.1073/pnas.96.6.2958.
[38] S. Benko, J.G. Magalhaes, D.J. Philpott, S.E. Girardin, NLRC5 limits the activation of inflammatory pathways, J. Immunol. 185 (2010) 1681–1691, https://doi.org/10.4049/jimmunol.0903900.
[39] J.M. Recla, R.F. Robledo, D.M. Gatti, C.J. Bult, G.A. Churchill, E.J. Chesler, Precise genetic mapping and integrative bioinformatics in diversity outbred mice reveals Hydin as a novel pain gene, Mamm. Genome 25 (2014) 211–222, https://doi.org/10.1007/s00335-014-9508-0.
[40] S. Smith, L. Bernatchez, L.B. Beheregaray, RNA-seq analysis reveals extensive transcriptional plasticity to temperature stress in a freshwater fish species, BMC Genomics 14 (2013), https://doi.org/10.1186/1471-2164-14-375.
[41] M.A. Febbraio, Alterations in energy metabolism during exercise and heat stress, Sports Med. 31 (2001) 47–59, https://doi.org/10.2165/00007256-200131010-00004.
[42] S. Akamine, S. Okuzono, H. Yamamoto, D. Setoyama, N. Sagata, M. Ohgidani, T. A. Kato, T. Ishitani, H. Kato, K. Masuda, Y. Matsushita, H. Ono, Y. Ishizaki, M. Sanefuji, H. Saitsu, N. Matsumoto, D. Kang, S. Kanba, Y. Nakabeppu, Y. Sakai, S. Ohga, GNAO1 organizes the cytoskeletal remodeling and firing of developing neurons, FASEB J. 34 (2020) 16601–16621, https://doi.org/10.1096/fj.202001113R.
[43] F. Huang, J. Chen, R. Lan, Z. Wang, R. Chen, J. Lin, L. Fu, Hypoxia induced δ-catenin to enhance mice hepatocellular carcinoma progression via Wnt signaling, Exp. Cell Res. 374 (2019) 94–103, https://doi.org/10.1016/j.yexcr.2018.11.011.
[44] Y. Wang, Y. Yang, Y. Yang, Y. Dang, Z. Guo, Q. Zhuang, X. Zheng, F. Wang, N. Cheng, X. Liu, W. Guo, B. Zhao, Hypoxia induces hepatocellular carcinoma metastasis via the HIF-1α/METTL16/lnc-CSMD1-7/RBFOX2 axis, IScience 26 (2023) 108495, https://doi.org/10.1016/j.isci.2023.108495.
[45] C.S. Cencer, J.B. Silverman, L.M. Meenderink, E.S. Krystofiak, B.A. Millis, M. J. Tyska, Adhesion-based capture stabilizes nascent microvilli at epithelial cell junctions, Dev. Cell 58 (2023) 2048–2062, e7, https://doi.org/10.1016/j.devcel.2023.09.001.
[46] D.F. Fiol, S.K. Mak, D. Kültz, Specific TSC22 domain transcripts are hypertonically induced and alternatively spliced to protect mouse kidney cells during osmotic stress, FEBS J. 274 (2007) 109–124, https://doi.org/10.1111/j.1742-4658.2006.05569.x.
[47] S. Yang, D. Li, L. Feng, C. Zhang, D. Xi, H. Liu, C. Yan, Z. Xu, Y. Zhang, Y. Li, T. Yan, Z. He, J. Wu, Q. Gong, J. Du, X. Huang, X. Du, Transcriptome analysis reveals the high temperature induced damage is a significant factor affecting the osmotic function of gill tissue in Siberian sturgeon (*Acipenser baerii*), BMC Genomics 24 (2023) 2, https://doi.org/10.1186/s12864-022-08969-9.
[48] C. Chen, J. Yuan, G. Ji, S. Zhang, Z. Gao, Amphioxus ribosomal proteins RPS15, RPS18, RPS19 and RPS30-precursor act as immune effectors via killing or agglutinating bacteria, Fish Shellfish Immunol. 118 (2021) 147–154, https://doi.org/10.1016/j.fsi.2021.09.001.
[49] I.-C. Su, Y. Su, H. Chuang, V.K. Yadav, S.A. Setiawan, I.-H. Fong, C.-T. Yeh, H.-C. Huang, C.-M. Lin, Ubiquitin-specific protease 6 n-terminal-like protein (USP6NL) and the epidermal growth factor receptor (EGFR) signaling Axis regulates ubiquitin-mediated DNA repair and Temozolomide-resistance in glioblastoma, Biomedicines 10 (2022) 1531, https://doi.org/10.3390/biomedicines10071531.
[50] S. Maksour, N. Ng, A.J. Hulme, S. Miellet, M. Engel, S.S. Muñoz, R. Balez, B. Rollo, R.K. Finol-Urdaneta, L. Ooi, M. Dottori, REST and RCOR genes display distinct expression profiles in neurons and astrocytes using 2D and 3D human pluripotent stem cell models, Heliyon 10 (2024) e32680, https://doi.org/10.1016/j.heliyon.2024.e32680.
[51] K. Sugiyama, H. Shimano, M. Takahashi, Y. Shimura, A. Shimura, T. Furuya, R. Tomabechi, Y. Shirasaka, K. Higuchi, H. Kishimoto, K. Inoue, The use of Carboxyfluorescein reveals the transport function of MCT6/SLC16A5 associated with CD147 as a chloride-sensitive organic anion transporter in mammalian cells, J. Pharm. Sci. 113 (2024) 1113–1120, https://doi.org/10.1016/j.xphs.2023.12.023.
[52] A. Nascimento, C. Bruels, A. Codina, J. Milisenda, C. Li, L. Carrera-García, E. Estrella, J. Pijuan, J. Expósito-Escudero, S. Stafki, L. Martorell, H. Lidov, C. Ortez, F. Palau, B. Darras, C. Jou, L. Kunkel, J. Hoenicka, P. Kang, D. Natera-de Benito, FP.36 Genetic variants in DTNA cause a mild dominantly inherited muscular dystrophy, Neuromuscul. Disord. 32 (2022) S113, https://doi.org/10.1016/j.nmd.2022.07.296.
[53] C. Church, C. Chapon, R.O. Poyton, Cloning and characterization of PET100, a gene required for the assembly of yeast cytochrome c oxidase, J. Biol. Chem. 271 (1996) 18499–18507, https://doi.org/10.1074/jbc.271.31.18499.
[54] S.J. Monkley, C.A. Pritchard, D.R. Critchley, Analysis of the mammalian Talin2 gene TLN2, Biochem. Biophys. Res. Commun. 286 (2001) 880–885, https://doi.org/10.1006/bbrc.2001.5497.
[55] M. Luo, W. Zhu, Z. Liang, B. Feng, X. Xie, Y. Li, Y. Liu, X. Shi, J. Fu, L. Miao, Z. Dong, High-temperature stress response: insights into the molecular regulation of American shad (*Alosa sapidissima*) using a multi-omics approach, Sci. Total Environ. 916 (2024) 170329, https://doi.org/10.1016/j.scitotenv.2024.170329.
[56] S.R. Geange, P.A. Arnold, A.A. Catling, O. Coast, A.M. Cook, K.M. Gowland, A. Leigh, R.F. Notarnicola, B.C. Posch, S.E. Venn, L. Zhu, A.B. Nicotra, The thermal tolerance of photosynthetic tissues: a global systematic review and agenda for future research, New Phytol. 229 (2021) 2497–2513, https://doi.org/10.1111/nph.17052.
[57] D.J. Barshis, J.T. Ladner, T.A. Oliver, F.O. Seneca, N. Traylor-Knowles, S. R. Palumbi, Genomic basis for coral resilience to climate change, Proc. Natl. Acad. Sci. 110 (2013) 1387–1392, https://doi.org/10.1073/pnas.1210224110.
[58] S.S.U.H. Kazmi, Y.Y.L. Wang, Y.-E. Cai, Z. Wang, Temperature effects in single or combined with chemicals to the aquatic organisms: an overview of thermo-chemical stress, Ecol. Indic. 143 (2022) 109354, https://doi.org/10.1016/j.ecolind.2022.109354.
[59] J.R. Lepock, How do cells respond to their thermal environment? Int. J. Hyperth. 21 (2005) 681–687, https://doi.org/10.1080/02656730500307298.